Time-Resolved Visual Chiral Discrimination of Cysteine Using Unmodified CdTe Quantum Dots

SCIENTIFIC REPORTS

OPEN

Time-Resolved Visual Chiral Discrimination of Cysteine Using Unmodified CdTe Quantum Dots

Received: 19 December 2016
Accepted: 17 March 2017
Published online: 18 April 2017

Forough Ghasemi[1], M. Reza Hormozi-Nezhad[1,2] & Morteza Mahmoudi[3,4]

Herein, we demonstrate a simple yet novel luminescence assay for visual chiral discrimination of cysteine. Thioglycolic acid (TGA)-capped cadmium-telluride (CdTe) quantum dots (QDs) exposing green emission were directly synthesized in aqueous solution. The interaction between cysteine molecules and CdTe QDs induced the aggregation of QDs via hydrogen bonding. As a result of electronic coupling within these aggregates, a redshift both in the absorption and emission spectra of QDs occured. The difference in the kinetics of the interactions between L- and D-cysteine with CdTe QDs led to chiral recognition of these enantiomers. Addition of D-cysteine to CdTe QDs in a basic media caused a green-to-yellow color change, while no color alteration in QDs emission was observed in the presence of L-cysteine after 2 hours. Notably, the QDs used in the proposed assay are free from any labling/modification, which makes the present strategy highly attractive for sensing applications. Furthermore, the presented chiral assay is able to determine the enantiomeric excess (ee) of D-cysteine in the whole range of ee values (from −100% to 100%).

Chirality is known as a determinative feature in biological phenomena. Many drugs, bioactive compounds and organic molecules exist in chiral form. In general, two enantiomers of a chiral compound exhibit different biochemical activity, pharmaceutical and physiological effects, depending on their absolute configurations[1–4]. Enantiomeric recognition of amino acids, as essential bioactive substances and building blocks of proteins, polypeptides, and various drugs, is of vital importance in both process development and quality control[5–7].

Various methods have been reported to distinguish the chirality of amino acids, including high performance liquid chromatography[8–10], gas chromatography[11], mass spectrometry[12], electrochemistry[13–15], and capillary electrophoresis[16,17]. However, most of these techniques require complicated sample pretreatment and sophisticated instrumentation which makes them impractical for real-time analysis. Rapid enantiosensing technique, *i.e.*, circular dichroism (CD), suffers from low sensitivity and low tolerance against contamination[18]. Thus, it is intriguing and useful to develop a rapid, simple, sensitive, and high-throughput assay especially, a solution-based sensor capable of visual discrimination of enantiomers. Colorimetric and fluorometric assays are highly demanded due to their ease of detection, even by naked eye and without the need of elaborate equipment.

Due to their unique optical properties, quantum dots (*e.g.*, cadmium-telluride (CdTe) QDs)[19], gold, and silver nanoparticles[20,21] possess a tremendous potential for applications in optical sensing. Reported colorimetric and fluorimetric chiral recognition probes for amino acids are based on either the inherent chirality of metal surfaces[22–24] or chiral molecules adsorbed on the nanoparticle surface[7,25–30]. Metallic nanoparticles with intrinsic chiral structure are numerable and the adsorption of chiral molecules onto the surface of nanoparticles leads to complex chiral detection.

In the present study we report a new strategy for chiral recognition in aqueous solution using CdTe QDs. We show that both D- and L-cysteine induce aggregation in CdTe QDs, but with different kinetics leading to distinct emission spectra and color change (see Fig. 1).

[1]Department of Chemistry, Sharif University of Technology, Tehran, 11155-9516, Iran. [2]Institute for Nanoscience and Nanotechnology, Sharif University of Technology, Tehran, Iran. [3]Department of Nanotechnology and Nanotechnology Research Center, Faculty of Pharmacy, Tehran University of Medical Sciences, Tehran, 13169-43551, Iran. [4]Department of Anesthesiology, Brigham and Women's Hospital, Harvard Medical School, Boston, Massachusetts, 02115, United States. Correspondence and requests for materials should be addressed to M.R.H. (email: hormozi@sharif.edu) or M.M. (email: mmahmoudi@bwh.harvard.edu)

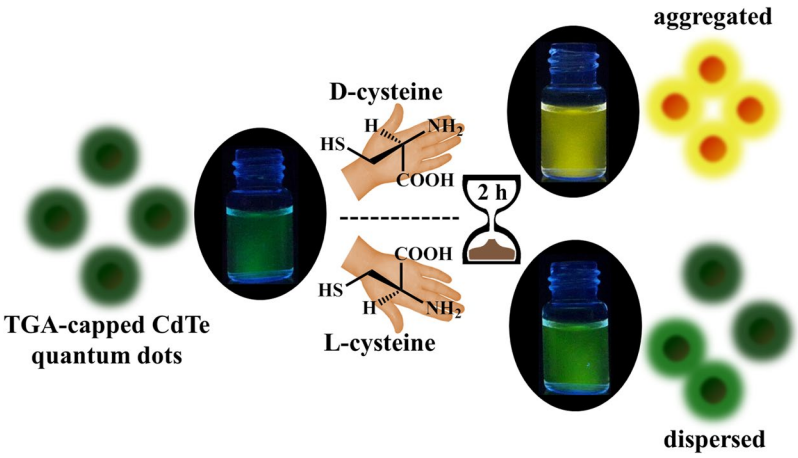

Figure 1. Schematic illustration of time-resolved visual chiral discrimination of cysteine using unmodified CdTe quantum dots.

Results and Discussion

Time-resolved chiral recognition. TGA-capped CdTe QDs exposing green emission were directly synthesized in aqueous solution. The absorption and fluorescence spectra of the as-prepared thioglycolic acid (TGA)-capped CdTe QDs are demonstrated in Fig. S1 in Supporting Information (SI). L- and D-cysteine were added to the QDs' solution and after 15 min NaOH was inserted to the mixture. Time-course emission behavior of QDs toward D- and L-cysteine is shown in Fig. 2. The emission of QDs was quenched thoroughly upon the addition of cysteine in the basic media. Recovery in fluorescence-intensity and redshift of the spectral peak were thereafter observed. In the case of L-cysteine, the fluorescence intensity reached a maximum value after 138 min with an intensity very close to the emission of the blank (solution with no cysteine, shown in Fig. S2). However, for D-cysteine, it took 78 min to obtain the maximal fluorescence intensity which was twice as high as the blank. In both cases, after reaching a maximum, fluorescence quenching and further redshift in the emission peak were observed.

As shown in Fig. 2, the presence of cysteine in solution triggered fluorescence quenching which can be attributed to the photoinduced electron transfer (PET)[31]. Unprotonated amino groups are particularly suitable as electron donors in PET mechanism[32]. Therefore, in the presence of cysteine, containing an amino unit, PET can take place between the nitrogen lone pair and QDs, causing quenching (see Fig. 3).

Due to the high binding affinity of thiol groups toward Cd atoms at the surface of CdTe QDs, cysteine can attach to CdTe through the formation of Cd-S bonds[33,34]. Therefore, after the addition of cysteine to QDs solution, cysteine was gradually bonded to the surface of QDs. It is assumed that the affinity of thiol to QDs can actually push the amino group away from the surface of QDs. Thus, considering the strong dependency of PET on the electron donor–fluorophore distance[32], PET was suppressed and allowed the fluorescence to be switched on (see Fig. 3).

The rate of fluorescence-intensity recovery by D-cysteine was faster than by L-cysteine. In addition, a higher fluorescence-intensity was observed for D-cysteine (see Fig. 2). Compared to L-cysteine, D-cysteine exhibits a stronger interaction affinity to CdTe QDs[34]. Consequently, it is expected that a higher number of D-cysteine compounds can attach to the surface of QDs, which caused enhancement in both the rate of recovery and the emission (due to better passivation of the QDs' surface)[35,36].

As demonstrated in Fig. 2, the redshift in the emission spectra was initiated upon the entrance of cysteine in the basic media. The presence of cysteine molecules on the surface of QDs induced the aggregation process due to the hydrogen bonding between the adsorbed thiols. Aggregation of QDs then caused a redshift in the emission spectra that can be explained by two possible reasons: (1) electronic coupling between neighbouring QDs in the aggregates which can lead to a redshift in both absorption and emission spectra; (2) exciton energy transfer between QDs in small distance which will not exhibit any redshift in the absorption spectra[37]. The observed redshift in the absorption spectra, cuased by the aggregation of QDs in the presence of cysteine (see Fig. S4), confirms that the redshift appeared in the emission spectra can be originated from electronic coupling between QDs.

Another point to be considered from Fig. 2 is that CdTe QDs displayed a gradual quenching after reaching a maximum emission intensity. In agreement with our findings, Koole *et al.*[37] had reported that exciton energy transfer is absent in small green QDs, while it can occur in aggregated QDs. Furthermore, a reduction in fluorescence intensity can be induced by exciton energy transfer[37]. Over time, the size and the number of aggregates increases which leads to exciton energy transfer between QDs in one aggregate, and consequently causes emission quenching.

Figure 4 illustrates the peak wavelengths related to the spectra given in Fig. 2, against time. In a certain time, the amount of redshift caused by D-cysteine was more than by L-cysteine. As mentioned earlier, the aggregation of QDs caused redshift in the emission spectra. Therefore, we hypothesized that the rate of aggregation is higher in the presence of D-cysteine, rather than L-cysteine. This can be used for visual discrimination between L- and D- forms of cysteine (see inset in Fig. 4). Over time, the difference in redshifts of QDs declined for both D- and

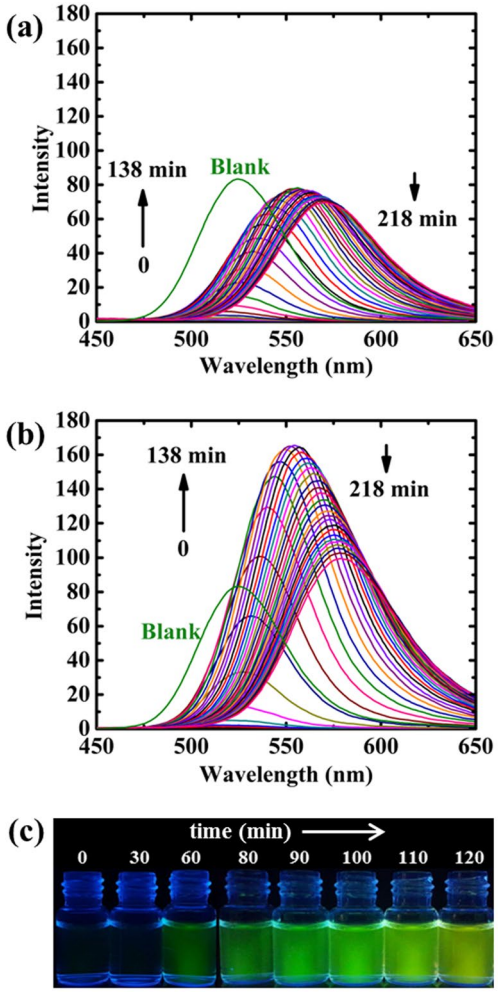

Figure 2. Time-course variation in emission spectra of CdTe QDs upon the addition of (**a**) L-cysteine and (**b**) D-cysteine (The concentrations of cysteine, NaOH, and QDs were 2 mmol L^{-1}, 60 mmol L^{-1}, and 4.6 μmol L^{-1}, respectively; the excitation wavelength was 340 nm, time interval to record each spectrum was 6 min). (**c**) Fluorescence images of time-dependent luminescence of QDs after the addition of 2 mmol L^{-1} D-cysteine and 60 mmol L^{-1} NaOH under UV irradiation, the time of the images was from 0 min (left) to 120 min (right).

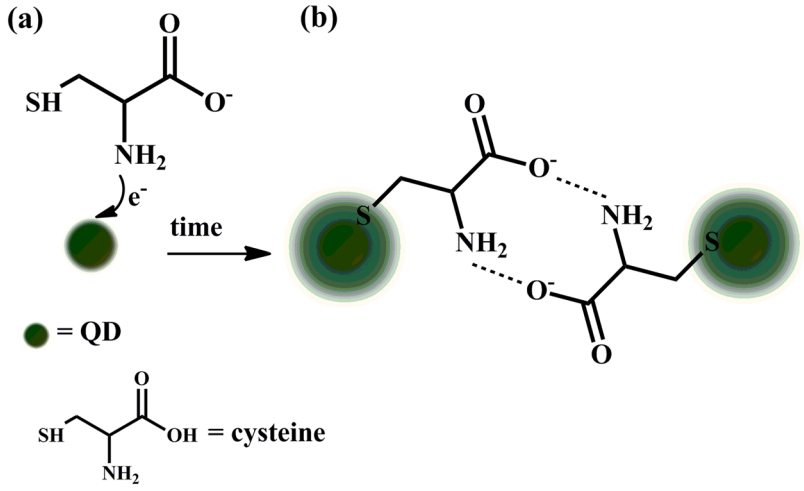

Figure 3. (**a**) Photoinduced electron transfer (PET)-mediated quenching of QD. (**b**) Fluorescence recovery of QDs by PET inhibition.

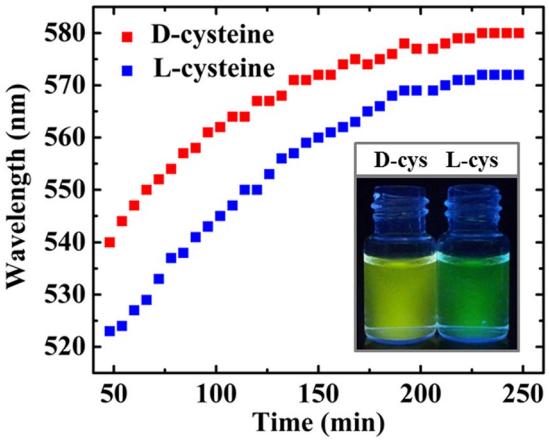

Figure 4. Changes in the wavelength of maximum fluorescence after the addition of D- and L-cysteine (2 mmol L^{-1}) against time (min). The inset shows fluorescence images of QDs 2 h after the addition of 2 mmol L^{-1} L-, D-cysteine and 60 mmol L^{-1} NaOH under UV irradiation.

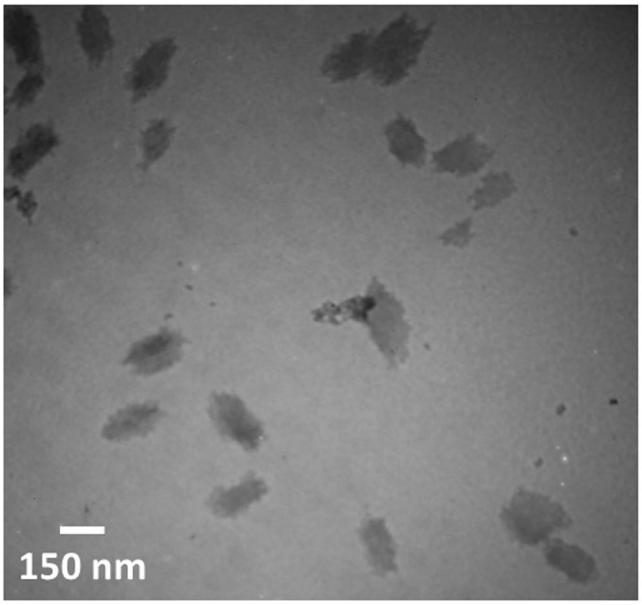

Figure 5. TEM images of CdTe QDs in the presence of D-cysteine.

L-cysteine. Dynamic light scattering (DLS) measurements confirm that D-cysteine mediates more aggregated QDs compared to L-cysteine (See Fig. S5). TEM images further confirmed the aggregation of QDs in the presence of cysteine (see Fig. 5). Figure 2c shows representative emitted colors from QDs over time after the addition of D-cysteine and NaOH under UV irradiation.

Fluorometric determination of enantiomeric excess. Since it is essential to determine enantiomeric excess (*i.e.*, the difference between the mole fractions of enantiomers) in chiral drug and asymmetric catalyst development[38,39], our chiral assay was applied to quantify the enantiomeric excess of cysteine. NaOH concentration, as an effective parameter on emission, was optimized. The difference between peak wavelengths of QDs' emission in the presence of D- and L-cysteine ($\Delta\lambda_{D,L}$) was monitored at different concentrations of NaOH (see Fig. S6). $\Delta\lambda_{D,L}$ rised up to 60 mmol L^{-1}, and then no further change was observed. Therefore, we selected 60 mmol L^{-1} of NaOH as the optimal concentration for further experiments. The emission spectra of CdTe QDs in different enantiomeric excess of cysteine (total concentration 1 mmol L^{-1}) are demonstrated in Fig. 6. The highest and lowest signals were observed for absolute D- and L-cysteine, respectively. A good linear relationship was obtained between emission signal at 530 nm and enantiomeric excess of D-cysteine.

The response of unmodified CdTe QDs to other α-amino acids. The response of the unmodified CdTe QDs in the presence of other α-amino acids including arginine, tryptophan, tyrosine, proline, and histidine was negligible regrdless to their D- and L- forms (see Fig. 7). However, the response of D-cysteine was the

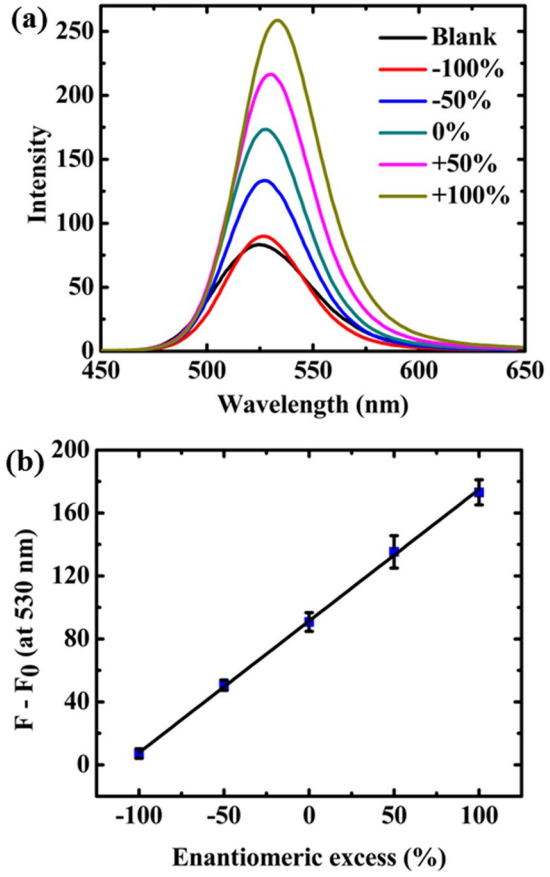

Figure 6. (**a**) Emission spectra of QDs in different enantiomeric excess of D-cysteine (the total concentration of cysteine was 1 mmol L^{-1}). (**b**) The relationship between fluorescence intensity and enantiomeric excess of D-cysteine at total cysteine concentration of 1 mmol L^{-1}.

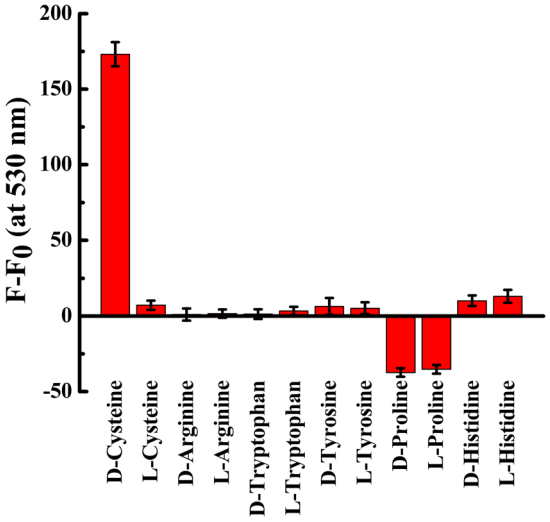

Figure 7. The responses of QDs to enantiomerically pure cysteine, arginine, tryptophan, tyrosine, proline and histidine amino acids at a concentration of 1 mmol L^{-1} (in the presence of 60 mmol L^{-1} NaOH).

highest and distinct from L-cysteine. All α-amino acids consist of a carboxylic acid and an amino functional group. However, cysteine is distinctive from the rest due to the presence of its thiol group. Considering that a chiral CdTe QD was employed in the proposed assay, the key role of the thiol group in the differentiation of L- and D-cysteine is evident. In fact, both D- and L-cysteine are bonded to the surface of QDs through S-Cd bond,

but with a different strength that makes them distinguishable. The CD measurement (Fig. S7) confirmed that the applied CdTe QDs were achiral. Similarly, the CD spectra of L- and D-cysteine exhibited mirror-image profiles (see Fig. S8). Aditional CD features emerged for the mixture of QDs and cysteine, compared to pure cysteine (see Fig. S9). These features can be attributed to the formation of $Cd_x(cystine)_y$ complex and to the chirality induced by the absorbed cysteine molecules on QDs surface[34]. This assumption has been experimentally and theoretically proven by Zhou *et al.*[34] studying CdTe QDs: since an atom with four different substituents produces a chiral center, if all four atomic positions in a tetrahedron formed by Te and Cd atoms are different, a chiral center will be formed. As they have presented, the adsorption of cysteine molecules on the surface of QDs induces four different substituents, resulting in a chiral center.

Conclusions

In summary, a fluorometric chiral recognition assay was developed for detection of cysteine using unmodified CdTe QDs. We found that the rate of QDs' aggregation was quite different in the presence of D- and L-cysteine. The chiral assay took advantage of the aggregation rate of unmodified QDs for enantioselective recognition of cysteines. The emission color variation of QDs revealed its promissing chiral detection of cysteine even by the naked eye. Moreover, this novel chiral sensor can be applied for the measurement of enantiomeric excess. Compared with other developed fluorimetric methods, the present strategy is fascinating mainly because the CdTe QDs employed do not require any labeling or modification with chiral molecules.

Methods

Reagents. Cysteine and other amino acids were purchased from Merck. Tellurium powder (Te), thioglycolic acid (TGA), Sodium borohydride ($NaBH_4$), and cadmium chloride ($CdCl_2.2H_2O$) were purchased from Sigma. Deionized water was used throughout the experiment.

Instrumentation. Absorbance spectra were recorded on a Lambda spectrophotometer from Perkin Elmer using 1.0 cm glass cell. The fluorescence spectra were measured on a Cary Eclipse fluorescence spectrometer (Varian) with the use of 1×1 cm quartz cell. All the spectra were recorded at room temperature. Size distributions were obtained using Zetasizer Viscotec 802 at ambient temperature. Circular dichroism (CD) measurements were made using Jasco J-810 CD recorder.

Synthesis of TGA functionalized CdTe QDs. TGA-capped CdTe QDs were prepared according to the procedure described previously (Ghasemi *et al.* 2016[40]). Typically, 2.87 mmol of TGA was added to 10 mL of $CdCl_2$ solution (0.29 mol L^{-1}) and the pH was adjusted to 9.0 with NaOH solution. Then, the solution was stirred under argon bubbling for 5 min. 0.76 mmol of Te powder was separately mixed with 75 mL of $NaBH_4$ solution (64 mmol L^{-1}) under argon flow at 50 °C. After 20 min, 10 mL of pH-adjusted $CdCl_2$ solution was added, and the temperature was increased to 150 °C. The resulting TGA-capped CdTe QDs with green emission (reaction time 45 min) were taken out and allowed to cool in ice bath.

References

1. Drayer, D. E., Wainer, I. & Drayer, D. Drug Stereochemistry, Analytical Methods and Pharmacology Vol. 209, Ch. 1 (Marcel Dekker, New York, 1988).
2. Hao, H., Wang, G. & Sun, J. Enantioselective pharmacokinetics of ibuprofen and involved mechanisms. *Drug Metab. Rev.* **37**, 215–234, doi:10.1081/DMR-200047999 (2005).
3. Mori, K. Significance of chirality in pheromone science. *Biorg. Med. Chem.* **15**, 7505–7523, doi:10.1016/j.bmc.2007.08.040 (2007).
4. Smith, S. W. Chiral toxicology: it's the same thing… only different. *Toxicol. Sci.*, kfp097 (2009).
5. Bera, S., Mondal, D., Singh, M. & Kale, R. K. Advances in serinals for asymmetric synthesis. *Tetrahedron* **69**, 969–1011, doi:10.1016/j.tet.2012.11.054 (2013).
6. Wu, G. Amino acids: metabolism, functions, and nutrition. *Amino Acids* **37**, 1–17, doi:10.1007/s00726-009-0269-0 (2009).
7. Han, C. & Li, H. Chiral Recognition of Amino Acids Based on Cyclodextrin-Capped Quantum Dots. *Small* **4**, 1344–1350, doi:10.1002/smll.v4:9 (2008).
8. Ilisz, I., Aranyi, A., Pataj, Z. & Péter, A. Enantiomeric separation of nonproteinogenic amino acids by high-performance liquid chromatography. *Journal of Chromatography A* **1269**, 94–121, doi:10.1016/j.chroma.2012.07.011 (2012).
9. Tang, M., Zhang, J., Zhuang, S. & Liu, W. Development of chiral stationary phases for high-performance liquid chromatographic separation. *TrAC Trends in Analytical Chemistry* **39**, 180–194, doi:10.1016/j.trac.2012.07.006 (2012).
10. Ilisz, I., Aranyi, A. & Péter, A. Chiral derivatizations applied for the separation of unusual amino acid enantiomers by liquid chromatography and related techniques. *Journal of Chromatography A* **1296**, 119–139, doi:10.1016/j.chroma.2013.03.034 (2013).
11. Jiang, Z., Crassous, J. & Schurig, V. Gas-chromatographic separation of tri (hetero) halogenomethane enantiomers. *Chirality* **17**, 488–493, doi:10.1002/chir.20191 (2005).
12. Yao, Z.-P., Wan, T. S., Kwong, K.-P. & Che, C.-T. Chiral analysis by electrospray ionization mass spectrometry/mass spectrometry. 1. *Chiral recognition of 19 common amino acids. Analytical chemistry* **72**, 5383–5393 (2000).
13. Doménech, A. & Alarcón, J. Microheterogeneous electrocatalytic chiral recognition at monoclinic vanadium-doped zirconias: enantioselective detection of glucose. *Analytical chemistry* **79**, 6742–6751, doi:10.1021/ac070623w (2007).
14. Kothari, H. M. *et al.* Enantiospecific electrodeposition of chiral CuO films from copper (II) complexes of tartaric and amino acids on single-crystal Au (001). *Chem. Mater.* **16**, 4232–4244, doi:10.1021/cm048939x (2004).
15. Fu, Y. *et al.* A new strategy for chiral recognition of amino acids. *Chemical Communications* **48**, 2322–2324, doi:10.1039/c2cc17301h (2012).
16. Lammers, I., Buijs, J., van der Zwan, G., Ariese, F. & Gooijer, C. Phosphorescence for sensitive enantioselective detection in chiral capillary electrophoresis. *Analytical chemistry* **81**, 6226–6233, doi:10.1021/ac900750e (2009).
17. Waldhier, M. C., Gruber, M. A., Dettmer, K. & Oefner, P. J. Capillary electrophoresis and column chromatography in biomedical chiral amino acid analysis. *Anal. Bioanal. Chem.* **394**, 695–706, doi:10.1007/s00216-009-2792-y (2009).
18. Bodoki, E., Oltean, M., Bodoki, A. & Ştiufiuc, R. Chiral recognition and quantification of propranolol enantiomers by surface enhanced Raman scattering through supramolecular interaction with β-cyclodextrin. *Talanta* **101**, 53–58, doi:10.1016/j.talanta.2012.09.001 (2012).
19. Freeman, R. & Willner, I. Optical molecular sensing with semiconductor quantum dots (QDs). *Chemical Society Reviews* **41**, 4067–4085, doi:10.1039/c2cs15357b (2012).

20. Jans, H. & Huo, Q. Gold nanoparticle-enabled biological and chemical detection and analysis. *Chemical Society Reviews* **41**, 2849–2866, doi:10.1039/c1cs15280g (2012).
21. Rycenga, M. *et al*. Controlling the synthesis and assembly of silver nanostructures for plasmonic applications. *Chemical reviews* **111**, 3669–3712, doi:10.1021/cr100275d (2011).
22. Wattanakit, C. *et al*. Enantioselective recognition at mesoporous chiral metal surfaces. *Nature communications* **5** (2014).
23. Zhang, L., Xu, C., Liu, C. & Li, B. Visual chiral recognition of tryptophan enantiomers using unmodified gold nanoparticles as colorimetric probes. *Analytica chimica acta* **809**, 123–127, doi:10.1016/j.aca.2013.11.043 (2014).
24. Liu, C., Li, B. & Xu, C. Colorimetric chiral discrimination and determination of enantiometric excess of D/L-tryptophan using silver nanoparticles. *Microchimica Acta* **181**, 1407–1413, doi:10.1007/s00604-014-1281-y (2014).
25. Su, H., Zheng, Q. & Li, H. Colorimetric detection and separation of chiral tyrosine based on N-acetyl-L-cysteine modified gold nanoparticles. *J. Mater. Chem.* **22**, 6546–6548, doi:10.1039/c2jm16746h (2012).
26. Xiong, D., Chen, M. & Li, H. Synthesis of para-sulfonatocalix [4] arene-modified silver nanoparticles as colorimetric histidine probes. *Chemical Communications*. 880–882, 10.1039/b716270g (2008).
27. Seo, S. H., Kim, S. & Han, M. S. Gold nanoparticle-based colorimetric chiral discrimination of histidine: application to determining the enantiomeric excess of histidine. *Analytical Methods* **6**, 73–76, doi:10.1039/C3AY41735B (2014).
28. Ou, J. *et al*. Electrochemical enantiorecognition of tryptophan enantiomers based on graphene quantum dots–chitosan composite film. *Electrochem. Commun.* **57**, 5–9, doi:10.1016/j.elecom.2015.04.004 (2015).
29. Ou, J., Zhu, Y., Kong, Y. & Ma, J. Graphene quantum dots/β-cyclodextrin nanocomposites: A novel electrochemical chiral interface for tryptophan isomer recognition. *Electrochem. Commun.* **60**, 60–63, doi:10.1016/j.elecom.2015.08.005 (2015).
30. Yu, Y. *et al*. An efficient chiral sensing platform based on graphene quantum dot–tartaric acid hybrids. *RSC Advances* **6**, 84127–84132, doi:10.1039/C6RA18477D (2016).
31. de Silva, A. P., Moody, T. S. & Wright, G. D. Fluorescent PET (Photoinduced Electron Transfer) sensors as potent analytical tools. *Analyst* **134**, 2385–2393, doi:10.1039/b912527m (2009).
32. Accetta, A., Corradini, R. & Marchelli, R. In *Luminescence Applied in Sensor Science* 175–216 (Springer, 2010).
33. Wang, G.-L., Dong, Y.-M., Yang, H.-X. & Li, Z.-J. Ultrasensitive cysteine sensing using citrate-capped CdS quantum dots. *Talanta* **83**, 943–947, doi:10.1016/j.talanta.2010.10.047 (2011).
34. Zhou, Y., Yang, M., Sun, K., Tang, Z. & Kotov, N. A. Similar topological origin of chiral centers in organic and nanoscale inorganic structures: effect of stabilizer chirality on optical isomerism and growth of CdTe nanocrystals. *Journal of the American Chemical Society* **132**, 6006–6013, doi:10.1021/ja906894r (2010).
35. Liu, F.-C., Cheng, T.-L., Shen, C.-C., Tseng, W.-L. & Chiang, M. Y. Synthesis of Cysteine-Capped Zn x Cd1-x Se Alloyed Quantum Dots Emitting in the Blue-Green Spectral Range. *Langmuir* **24**, 2162–2167, doi:10.1021/la702972d (2008).
36. Koneswaran, M. & Narayanaswamy, R. L-Cysteine-capped ZnS quantum dots based fluorescence sensor for Cu^{2+} ion. *Sensors and Actuators B: Chemical* **139**, 104–109, doi:10.1016/j.snb.2008.09.028 (2009).
37. Koole, R., Liljeroth, P., de Mello Donegá, C., Vanmaekelbergh, D. & Meijerink, A. Electronic coupling and exciton energy transfer in CdTe quantum-dot molecules. *Journal of the American Chemical Society* **128**, 10436–10441, doi:10.1021/ja061608w (2006).
38. Gawley, R. E. Do the terms "% ee" and "% de" make sense as expressions of stereoisomer composition or stereoselectivity? *The Journal of organic chemistry* **71**, 2411–2416, doi:10.1021/jo052554w (2006).
39. Pellissier, H. Recent developments in dynamic kinetic resolution. *Tetrahedron* **64**, 1563–1601, doi:10.1016/j.tet.2007.10.080 (2008).
40. Ghasemi, F., Hormozi-Nezhad, M. R. & Mahmoudi, M. Identification of catecholamine neurotransmitters using fluorescence sensor array. *Analytica Chimica Acta* **917**, 85–92 (2016).

Acknowledgements

The support of this research by the Sharif University of Technology Research Council is gratefully acknowledged.

Author Contributions

F.Gh. performed the chemical and biological experiments and analyzed the results by the guidance of M.R.H.-N. and M.M. as the supervisor.

Additional Information

Supplementary information accompanies this paper at doi:10.1038/s41598-017-00983-2

Competing Interests: The authors declare that they have no competing interests.

Publisher's note: Springer Nature remains neutral with regard to jurisdictional claims in published maps and institutional affiliations.